Surface Activity, SANS, and Viscosity Studies in Aqueous Solutions of Oxyethylene and Oxybutylene Di- and Triblock Copolymers

Saurabh S. Soni,[†] Nandhibatla V. Sastry,*[,†] Ajay K. Patra,[‡] Jayant V. Joshi,[§] and Prem S. Goyal[§]

Department of Chemistry, Sardar Patel University, Vallabh Vidyanagar−388 120, Gujarat, India, Solid State Physics Division, Bhabha Atomic Research Center, Mumbai−400 085, India, and Inter University Consortium (IUC) for DAE Facilities, Mumbai Center, Mumbai−400 085, India

Received: June 10, 2002; In Final Form: September 20, 2002

The surface active and association properties of diblock and triblock type, $E_{18}B_9$ and $E_{13}B_{10}E_{13}$, copolymers in aqueous solutions have been studied by surface tension, small angle neutron scattering, and viscosity methods. Various fundamental parameters such as critical micelle concentration, area per molecule at water/air interface, and the surface excess concentrations have been estimated. The thermodynamics of micellization has been monitored. Both copolymers micellize through close association processes and the micellization is found to be entropy driven. SANS analysis showed that micelles formed are spherical in shape at 30 °C and the micellar size and association number showed constancy in the concentration range (1−15 wt %) at 30 °C. However, raising the temperature distorted the micellar shape from spherical to prolate ellipsoidal, with large effects on the size and association number. The elongation of micelles and increase in association number have been attributed to their dehydration at elevated temperatures. Dilute solution viscosities have been used to estimate the hydration of micelles over a temperature range of 30−70 °C. The surface active and micellar properties have also been discussed in terms of architecture of block copolymers.

1. Introduction

The colloidal chemical aspects of hydrophobic−hydrophilic block copolymers in aqueous solution have received great attention because of their fundamental and practical importance. The academic interest has been mostly centered around studies on the micellization, surface activity, and gelation properties of triblock $E_mP_nE_m$ (E = oxyethylene and P = oxypropylene) copolymers, which are now commercially available. The association and related behavior of these familiar triblock copolymers are already well reviewed.[1−4] In contrast to the extensive literature available on triblock EPE copolymer aqueous solutions, relatively few studies on EP diblock copolymer aqueous solutions are made.[5−8] This is partly because until recently it was not possible to prepare pure samples of monodisperse EP diblock or EPE triblock copolymers.[1,8,9] The anionic polymerization of 1,2-butylene oxide, however, allows preparation of wide range of E_mB_n, $E_mB_nE_m$ and $B_nE_mB_n$ (where B = oxybutylene and E = oxyethylene) copolymers.[10−18] The association, surface-active, and gelation properties of this type of copolymers in aqueous solutions have been studied using dynamic and static light scattering and surface tension methods.[13−18]

It has been concluded that for E_mB_n and $E_mB_nE_m$ copolymers of comparable block length and composition, diblock copolymer micelles, (i) have larger size and association number and (ii) have lower critical micelle concentration than their triblock counterparts.[7,13−15,19] The micelles have, in general, been assumed to be spherical in shape and, at a given temperature, the micellar association number decreased and the micellar radii increased as the E block length increased.[19] The static and dynamic light scattering measurements on EB diblock copolymer micelles in aqueous solutions further indicated that the micellar association number gradually increased, while no major changes were noted in the hydrodynamic radius of micelles as the temperature increased.[18,20−22]

It is unclear from these studies whether the micelles retain their spherical shape at elevated temperatures, and also what happens to the intermicellar interactions at high temperatures close to the cloud point. In a recent small angle neutron scattering (SANS) study, Deric et al.[23] have examined dilute aqueous solutions (1 and 1.8 wt %) of a long E block containing $E_{90}B_{10}$ diblock copolymer. A model based on a homogeneous spherical micelle core with attached Gaussian chains was considered to extract parameters for understanding the structure of micelles and interactions within them. The authors have concluded that the micelles retain their spherical shape at elevated temperatures of 50 and 70 °C with a slight increase in core radius. The effective volume fraction of micelles showed a maximum in the temperature range of 20−70 °C and hence it was thought that at 70 °C, the effective attraction between the E units within and between the micelles was enhanced because of poor solvent quality of water at this temperature. Hamley et al.,[24] however, concluded from SANS measurements on 1 wt % solutions of $E_{18}B_{10}$ and $E_{40}B_{10}$ copolymers that both of the diblock copolymers form spherical micelles at 20 °C. But the rise in temperature was reported to have different effects on their micelles. The micelles of $E_{40}B_{10}$ retain the spherical shape at 60 °C with slight increase of 8 Å in micellar radius from 40 Å (at T = 20 °C). However, $E_{18}B_{10}$ spherical micelles (at T = 20 °C) started turning into straight cylinders with the latter flexible chains (worm like nature) in the temperature range of 40−50 °C. Thus the role of E block length seems to be crucial

* Corresponding author. E-mail: nvsastry_ad1@sancharnet.in
[†] Sardar Patel University.
[‡] Bhabha Atomic Research Center.
[§] Inter University Consortium.

10.1021/jp026277y CCC: $22.00
Published on Web 11/19/2002

in addressing the question of constancy of size and shape over temperature changes. It seems that the smaller the E block length, the greater will be the core enlargement at elevated temperatures. The role of molecular architecture, i.e., di- or triblock, on the temperature-induced structural changes in EB or EBE block copolymer micelles is yet to be studied.

In view of the scarce structural information on EB diblock copolymers and the nonavailability of such information on EBE copolymer micelles, the present study has been taken up to investigate in a detailed manner the association and surface active properties of di- and triblock EB and EBE copolymers (having identical B units) using surface tension, SANS, and viscosity studies. The effects of block architecture, concentration, and temperature on various surface-active properties and micellar parameters, viz. micellar size, shape, volume fraction and association number, etc., have been monitored and explained. We believe that the present study is the first of its kind dealing with analyzing the changes in micellar properties of a EB and EBE copolymer under identical conditions.

2. Experimental Section

2.1. Copolymers. The block copolymers were obtained as gift samples from The Dow Chemical Company, Freeport, Texas. They were used as received. The diblock copolymer BM−45 has a structure of type, MeO−$(EO)_m$−$(BO)_n$−OH with $m = 18$ and $n = 9$ units, while the triblock copolymer, B−40 has a structure HO−$(EO)_m$−$(BO)_n$−$(EO)_m$−OH with $m = 13$ and $n = 10$ units. EO and BO in the structures represent oxyethylene and oxybutylene units, and MeO denotes a methoxy group. The di- and triblock copolymers have been denoted as B-1 and B-2.

2.2. Methods. The surface tension of copolymer solutions was measured by the drop weight method using a modified stalagmometer.[25] The surface tensions calculated by this method agreed within ±0.2% of the values for pure organic liquids reported in the literature.[26]

The SANS experiments were carried out on micellar solutions prepared by dissolving known amounts of copolymers in D_2O and using a home-built SANS spectrometer at the DHRUVA Reactor, (Trombay, India).[27] The D_2O (with at least 99.5 atom % purity) was obtained from the heavy water division of BARC, Mumbai, India. The use of D_2O instead of H_2O for preparing the solutions provides a very good contrast between the associates of solute and the solvent in SANS experiments. The solutions were held in 0.5 cm path length UV-grade quartz sample holders with tight and fitting Teflon stoppers sealed with Parafilm. The sample to detector distance was 1.8 m for all runs. The spectrometer makes use of a BeO filtered beam and has a resolution ($\Delta Q/Q$) of about 30% at $Q = 0.05$ Å^{-1}. The angular distribution of the scattered neutron was recorded using a one-dimensional position-sensitive detector. The accessible wave transfer Q ($= 4\pi \sin 0.5\theta/\lambda$, where λ is the wavelength of the incident neutrons and θ is the scattering angle) range of this instrument is between 0.02 and 0.3 Å^{-1}. The mean neutron wavelength was $\lambda = 5.2$ Å.

The measured scattering intensities of neutrons were corrected for the background, empty cell scattering and sample transmission. The intensities then were normalized to absolute cross-section units.[27] Thus, plots of $d\Sigma/d\Omega$ vs Q were obtained. The uncertainty in the measured scattering intensities is estimated to be 10%. The experimental points are fitted using a nonlinear least-squares method.

The flow times of copolymer solutions and water were obtained by using Ubbelohde suspended level viscometers. Two viscometers were used to obtain flow times in the range of 130−360 s, thus avoiding any kinetic corrections. Three consecutive flow times, agreeing within ±0.02 s, were recorded and the mean flow time was considered. Shear corrections were not taken into consideration because obtained intrinsic viscosities were always less than 3 dL g^{-1}. The flow volume was greater than 5 mL, making drainage corrections unimportant. The viscometers during the measurements were suspended in thermostatic water baths maintained at constant temperature accurate to ±0.01 °C. The densities of aqueous copolymer solutions were measured using a high precision Anton Paar density meter DMA 5000. The measured densities are accurate to ±0.000001 g cm^{-3}, and the temperature control during the measurements has a precision of ±0.01 °C.

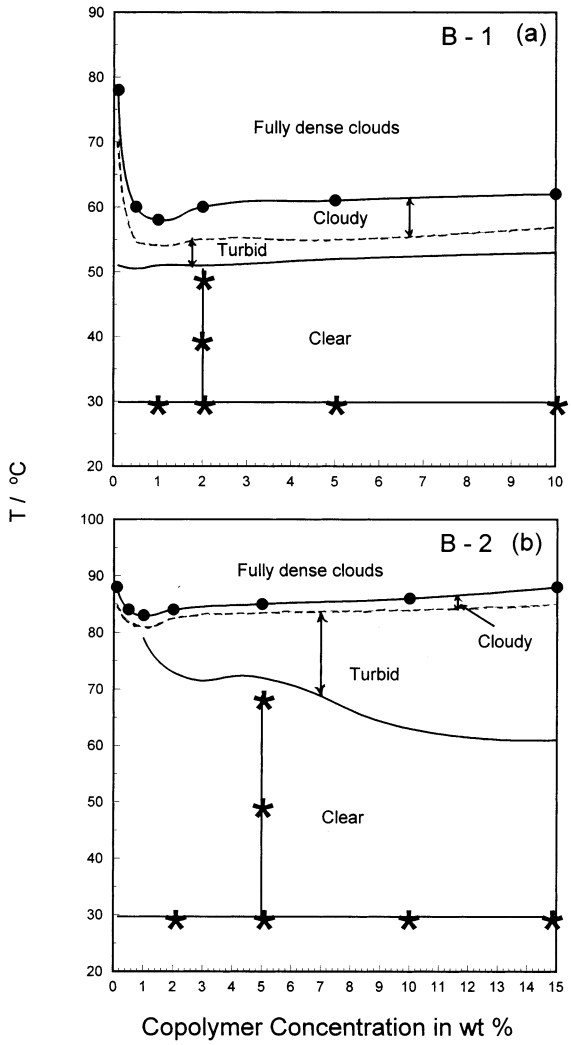

Figure 1. Phase diagrams for the copolymers (a) B-1 and (b) B-2 in dilute aqueous solutions; (●) final cloud point for copolymer solutions. Crosses on the horizontal line indicate the concentrations and on the vertical line indicate the temperatures corresponding to SANS and viscosity measurements.

3. Results and Discussion

3.1. Phase Diagrams. The phase diagrams for the dilute aqueous solutions of copolymers were constructed by visual examination of the change in the physical appearance of respective solutions with the temperature (see Figure 1a and b). The curves for both of the copolymers are characterized by a similar nature. The solutions in the concentration range (0.1−10 wt % for B-1 and 0.1−15 wt % for B-2) studied remain

TABLE 1: Values of CMC, CMC/C_{20}, Surface Excess Concentration, Γ_m, Area Per Copolymer Molecule, a_1^s, Maximum Surface Pressure, π_{CMC}, Free Energy, ΔG°_{mic}, Enthalpy, ΔH°_{mic}, and Entropy, ΔS°_{mic}, of Micellization for Copolymer Micelles

copolymer	temp (°C)	CMC (mol dm^{-3})	CMC/C_{20}	Γ_m ($\times 10^{10}$ mol cm^{-2})	a_1^s (Å^2)	π_{CMC} (mN m^{-1})	ΔG°_{mic} (kJ mol^{-1})	ΔH°_{mic} (kJ mol^{-1})	ΔS°_{mic} (kJ K^{-1} mol^{-1})
B-1	15	$2.6 \pm 0.2 \times 10^{-5}$	63	2.0 ± 0.1	85 ± 4	39 ± 2	-34.9 ± 1.5	14.9 ± 0.7	0.17
	25	$2.1 \pm 0.1 \times 10^{-5}$	32	2.2 ± 0.1	75 ± 6	38 ± 2	-36.6 ± 1.4	16.0 ± 0.9	0.18
	45	$1.4 \pm 0.1 \times 10^{-5}$	8	3.3 ± 0.2	51 ± 2	36 ± 1	-39.7 ± 1.3	18.2 ± 1.2	0.18
B-2	15	$3.0 \pm 0.2 \times 10^{-4}$	1406	1.5 ± 0.1	113 ± 2	46 ± 2	-29.1 ± 1.0	10.7 ± 0.5	0.13
	25	$2.2 \pm 0.2 \times 10^{-4}$	178	1.6 ± 0.1	102 ± 3	40 ± 2	-30.8 ± 1.1	11.4 ± 0.6	0.14
	45	$1.9 \pm 0.1 \times 10^{-4}$	15	2.1 ± 0.1	80 ± 2	35 ± 2	-33.3 ± 1.3	13.0 ± 0.8	0.15

isotropic and clear initially, then turn turbid before becoming cloudy at higher temperature. The clouds formed become more dense with further rise in temperature. The temperature at which dense clouds were noted is considered as the cloud point (Cp).

Our noted temperatures (for 1 wt % solution of copolymers) corresponding to initial turbidity (48 °C for B-1 and 79 °C for B-2) and cloud point (60 °C for B-1 and 83 °C for B-2) are in close agreement with the values of 48 °C and 79 °C; 57 °C and 83 °C for the same diblock and triblock copolymers, respectively.[7] The turbidity noted in the solutions indicates that the miscibility of the oxybutylene moiety with water worsens at elevated temperatures. The turbidity region is more for B-2 (triblock) than B-1 (diblock) (Figure 1a and b), because triblock copolymer has a over all longer water soluble E block.

3.2. Surface Tension Measurements. The surface tension method is versatile because it not only can estimate CMC values but also provides vital information about the adsorption characteristics of solutes at the air/water interface.[28] Plots of surface tension (γ) vs log C (where C is the concentration in wt %) at 15, 25, and 45 °C are shown in Figure 2a and b. For both copolymers, the surface tension values at all the three temperatures decrease linearly with the logarithm of the copolymer concentration and show a characteristic break beyond which the values remain almost constant. The CMC values were assigned to the break point interpolated of the two lines drawn through the data. The values of CMC for both copolymers are listed in Table 1. The CMC decreases with an increase in temperature. Our estimated CMC values of 2.1×10^{-5} and 2.2×10^{-4} mol dm^{-3} for B-1 and B-2 at 25 °C are in close agreement with the values of 2.3×10^{-5} and 2.1×10^{-4} mol dm^{-3} for the same copolymers.[7] However, our CMC values differ from those of 0.44, 0.37, and 0.25×10^{-4} mol dm^{-3} for the B-1 copolymer at 20, 30, and 40 °C reported recently by Kelarakis et al.[29] The authors have used a very sensitive surface tensiometer for measuring surface tension changes with more points around the CMC region. They have defined CMC as the concentration at which a constant value of the surface tension is obtained, in contrast to the interpolation method used by us. However, our observed γ_{CMC} values of 32.0 and 30.5 mN m^{-1} at 25 and 45 °C for the same copolymer lie between 32.5 and 31.5; 31.5 and 29.8 for the temperatures of 20 and 30 °C; 40 and 50 °C, as measured by Kelarakis et al.

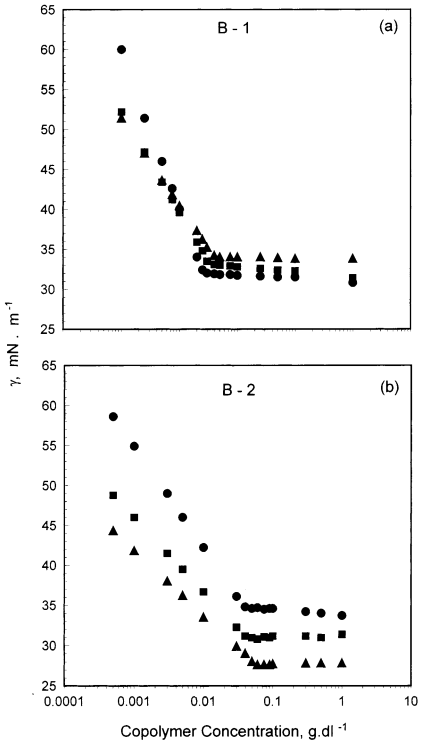

Figure 2. Plots of surface tension vs logarithm concentration for (a) B-1 and (b) B-2 copolymer aqueous solutions at different temperatures; (▲) 15 °C, (■) 25 °C, and (●) 45 °C.

Column 4 of Table 1 lists the CMC/C_{20} ratio values (where C_{20} is the concentration at which the surface tension of water is reduced by 20 mN m^{-1}). The B-2 copolymer has been found to have a ratio value of 178 (at 25 °C) in contrast to a smaller value of 32 for the B-1 copolymer. The larger the CMC/C_{20} value, the less will be the tendency of copolymer molecules to associate in solution. Hence, the noted higher CMC values for the B-2 copolymer over the B-1 copolymer are justified. The CMC/C_{20} values have been found to be decreased drastically for both copolymers with rise in temperature. Such strong temperature dependence of CMC/C_{20} values has also been reported for nonionic alkyl polyethers[28] and $E_mP_nE_m$ copolymers.[30]

The slope from the linear part of surface tension curves is related to surface excess concentration (Γ_m) of copolymer in the surface layer compared to the bulk, through the Gibbs adsorption isotherm:

$$\Gamma_m = -\frac{1}{2.303RT}\left(\frac{\partial\gamma}{\partial \log C}\right)_T \qquad (1)$$

Then one can estimate the area per molecule in the surface monolayer from the relation

$$a_1^s = \frac{10^{16}}{N_A \Gamma_m} \qquad (2)$$

where $R = 8.31$ J mol^{-1} K^{-1}, T = absolute temperature in K, $\partial\gamma/\partial \log C$ is the slope of the linear portion of the γ vs log C plots, N_A = Avogadro's number, and Γ_m is expressed in mol cm^{-2}. From the plots of Figure 2, one more quantity called the maximum surface pressure, π_{CMC}, can be estimated. π_{CMC} is the difference between the surface tension value of water and the value corresponding to the limiting region beyond the CMC. The values of Γ_m, a_1^s, and π_{CMC} are also listed in Table 1. It can be seen from the data that the area per diblock copolymer molecule in the surface monolayer is smaller than the same for a triblock copolymer molecule. Yang et al.[13] have also noted

smaller a_1^s values (2−3 times smaller) for the $E_{41}B_8$ than the $E_{21}B_8E_{21}$ copolymer. The a_1^s values systematically decreased with increase in temperature. Bedells et al.[20] have also reported a similar decrease in a_1^s values with increase in temperature for the $E_{50}B_{13}$ diblock copolymer at the air/water interface. The last three columns of Table 1 list various thermodynamic parameters, viz. free energy, $\Delta G°_{mic}$, enthalpy, $\Delta H°_{mic}$, and entropy, $\Delta S°_{mic}$, of micellization for both copolymers calculated using following relations derived from combination of pseudo-phase separation and mass action models:

$$\Delta G°_{mic} = RT \ln\left(\frac{CMC}{\omega}\right) \tag{3}$$

where ω is the molarity of water,

$$\Delta H°_{mic} = -RT^2\left(\frac{\partial \ln CMC}{\partial T}\right) \tag{4}$$

and

$$\Delta S°_{mic} = \frac{\Delta H°_{mic} - \Delta G°_{mic}}{T} \tag{5}$$

The $\Delta G°_{mic}$ values are always found to be negative and become more negative with rise in temperature from 15 to 45 °C. This indicates that the tendency of micellization increases with enhanced hydrophobicity of oxybutylene and oxyethylene units as a consequence of dehydration effects. Our estimated $\Delta G°_{mic}$ values of −36.6 and −30.8 kJ mol^{-1} for B-1 and B-2 copolymers agree with reported values of −36.4 and −30.4 kJ mol^{-1} for the same copolymers by Nace.[7] The $\Delta H°_{mic}$ values have been always found to be positive. Hence the observed $-\Delta G°_{mic}$ values have a predominant contribution from the positive $\Delta S°_{mic}$. It is further interesting to note that the $\Delta S°_{mic}$ for diblock copolymer micelles is slightly more positive than triblock copolymer micelles. Triblock copolymers of the type $E_mB_nE_m$ form micelles in water with the middle hydrophobic B part as the core and with the end E groups protruding into solution. The presence of E parts on both the ends of a EBE copolymer restricts the folding and thus the mobility of the B moiety, and hence micellization is expected to be less favorable in triblock copolymers than in diblock copolymers.

3.3. Small Angle Neutron Scattering (SANS). SANS measurements were used to construct the neutron scattering profiles for di- and triblock copolymer aqueous solutions under varying concentrations (1−10 wt % for B-1) and (2−15 wt % for B-2) at fixed temperature (30 °C) and for different temperatures at a fixed concentration (2 wt % for B-1 and 5 wt % for B-2). While carrying out SANS measurements, care has been taken to ensure that the solutions are transparent in appearance.

3.3.1. SANS Analysis. Calculation of the Scattering Intensity. For a monodisperse system of particles, the coherent differential scattering cross section, $d\Sigma/d\Omega$ can be written as[31,32]

$$\frac{d\Sigma}{d\Omega} = n_m V^2{}_m(\rho_m - \rho_s)^2 P(Q)S(Q) + B \tag{6}$$

The above expression can be simplified for noninteracting micelles (i.e., for dilute solutions, the interparticle structure factor $S(Q) \sim 1$) as

$$\frac{d\Sigma}{d\Omega} = n_m V^2{}_m(\rho_m - \rho_s)^2 P(Q) + B \tag{7}$$

where n_m denotes the number density of micelles, V_m is the micellar volume and ρ_m and ρ_s are scattering length densities of the micelles and solvent, respectively. $P(Q)$ is the single particle (intraparticle) structure factor, and $S(Q)$ is the interparticle structure factor. B is a constant term that represents the incoherent scattering from the background, which is mainly due to hydrogen in the sample.

For SANS experiments, the copolymer solutions were prepared in D_2O. The EB copolymeric micelles in water consisted of a hydrophobic polyoxybutylene (POB) core surrounded by a hydrophilic polyoxyethylene (POE) corona. The scattering length densities of POB block (0.212×10^{10} cm^{-2}) and D_2O (6.38×10^{10} cm^{-2}) have been used for calculation purposes. Thus, there is a very good contrast between the hydrophobic core and the solvent. However, because of the large amount of D_2O (water of hydration) present in the outer POE corona, the scattering contrast between the hydrated corona and the solvent is expected to be poor. In view of the above, as considered by others,[33,34] we also assume that P(Q) depends only on the hydrophobic core radius. The P(Q) for the spherical micellar core can be written as

$$P(Q) = \left[\frac{3}{(QR_c)^3}(\sin(QR_c) - QR_c\cos(QR_c))\right]^2 \tag{8}$$

where R_c is the hydrophobic core radius which is attributed to the size of the micellar core.

Structure Factor for Interacting Micelles. The interparticle structure factor $S(Q)$ depends on the spatial distribution of micelles. The scattering function shows a correlation peak when there is an increase in concentration, which reveals significant micelle−micelle interaction. The structure factor $S(Q)$ is given by[35]

$$S(Q) = 1 + 4\pi n \int (g(r) - 1)\frac{\sin(Qr)}{Qr} r^2\, dr \tag{9}$$

where $g(r)$ is the radial distribution function describing the arrangement of the micelles. If one assumes a hard-sphere nearest neighbor interaction potential between the micelles and the Percus−Yevick approximation[36] for describing direct correlation between two scattering objects, then the analytical form of the structure factor can be written as[37−39]

$$S(Q) = \frac{1}{1 + 24\phi G(2QR_{hs}, \phi)/(2QR_{hs})} \tag{10}$$

where R_{hs} is the hard sphere micellar radius, consisting of both POB and POE, and is the physical size of the micelle. ϕ is the hard sphere volume fraction of the micelles in the solution. G is a function of $x = 2QR_{hs}$ and ϕ: the ϕ value can mathematically be made equivalent to

$$C_m 4\pi R_{hs}{}^3 N_A/3N1000 \tag{11}$$

where C_m is the concentration of copolymer molecules in associated (micellized) form and has an unit in terms of mol dm^{-3}:

$$G(x,\phi) = (\alpha(\phi)/x^2)[\sin x - x\cos x] + (\beta(\phi)/x^3) \times [2x\sin x + (2 - x^2)\cos x - 2] + (\gamma(\phi)/x^5) \times \{-x^4\cos x + 4[(3x^2 - 6)\cos x + (x^3 - 6x)\sin x + 6]\}$$

where α, β, and γ are defined as

$$\alpha = (1 + 2\phi)^2/(1 - \phi)^4$$
$$\beta = -6\phi(1 + \phi/2)^2/(1 - \phi)^4$$
$$\gamma = (\phi/2)(1 + 2\phi)^2/(1 - \phi)^4$$

TABLE 2: Values of Core Radius, R_c, Hard Sphere Radius, R_{hs}, Micellar Volume Fraction, ϕ, Association Number, N, and Number Density, ζ, for the EB and EBE Copolymer Micelles in Aqueous Solution at 30 °C

conc (wt %)	R_c (Å)	R_{hs} (Å)	ϕ	N	ζ (cm^{-3})
		B-1			
1	44	100	0.015	340	1.104×10^{16}
2	43	98	0.028	318	2.368×10^{16}
5	43	99	0.048	318	7.350×10^{16}
10	43	98	0.088	318	17.110×10^{16}
		B-2			
2	35	70	0.024	154	0.408×10^{17}
5	34	69	0.045	142	1.219×10^{17}
10	34	69	0.066	142	3.600×10^{17}
15	34	68	0.116	142	6.015×10^{17}

Thus, in fitting experimental neutron scattering data from diblock and triblock copolymer solutions to eq 6, three unknown parameters, R_c, R_{hs}, and ϕ are encountered.

The association number, N, can be obtained from the knowledge of the core size

$$N = 4\pi(R_c)^3/3nV_{BO} \tag{12}$$

where n is the number of oxybutylene units in the POB block, R_c is the radius of the anhydrous core, and V_{BO} is the volume of one oxybutylene unit (116.5×10^{-24} cm^3). From the estimated values of N, the number density of micelles, ζ, i.e., the number of copolymer micelles per unit volume, is calculated by the following relation:

$$\zeta/\mathrm{cm}^{-3} = \frac{\mathrm{C} \times N_A \times 10^{-3}}{N} \tag{13}$$

where C = concentration in mol dm^{-3} and N_A = Avogadro's number.

All of the parameters that characterize the micellar associates of EB and EBE copolymers, as extracted from the above procedure, are listed in Table 2.

3.3.2. Concentration Dependence. SANS distributions as a function of copolymer concentration (C = 1, 2, 5, 10 wt % for B-1 and C = 2, 5, 10, 15 wt % for B-2) at 30 °C are shown in parts a and b of Figure 3. The intensity shows relatively strong Q dependence indicating that the copolymer molecules associate into micelles. The lower concentration used in SANS measurements is much greater than the CMC values of respective copolymers. A perusal of columns 2 and 3 of Table 2 reveals that the core radius, R_c, and hard sphere radius, R_{hs} literally do not vary in the concentration range of our study (1−10 wt % for B-1 and 1−15 wt % for B-2 copolymer). The micellar association number, as calculated by using eq 12, is also invariant within the above concentration range. The N values of 340 and 154 (for 1 wt % B-1 and 2 wt % B-2 copolymer solutions) are 7% and 9% higher than the rest of the values. The volume fraction of micelles however shows a gradual increase with the rise in concentration, indicating that more and more copolymer molecules associate into micelles. Our estimated R_c value of 44 Å for B-1 (at 1 wt % concentration) is comparable with the values of 45 Å (at 20 °C) for the same copolymer micelles as estimated from the SANS analysis of 1 wt % aqueous solution using a uniform sphere model.[24] The near constancy in the size and association number of micelles of the B-1 and B-2 copolymers (within the concentration range of 1−15 wt %) clearly indicates there is no change in the micellar structure under these conditions. Similar constancy in micellar association number, core radius, and hard sphere interaction radius for $E_{86}B_{10}$ micelles in aqueous solutions was also reported from SANS analysis of 1 and 1.8 wt % solutions using a model assuming a homogeneous spherical micelle core with attached Gaussian chains.[23] In short, our results are in good agreement with the available SANS studies on similar systems. It is seen, however, that our values of association number, N, are considerably higher than those obtained using light scattering techniques. For example, compared to our value of $N \sim 318$ for B-1 micelles at 30 °C, Yu et al.[15] obtained $N = 70$ and 110 at 25 °C and 40 °C, respectively. Again, SANS values of $N \sim 142$ for B-2 micelles at 30 °C is much higher than the light scattering values of $N = 13$ and 23 at 25 °C and 40 °C, respectively. We believe this is connected with the fact that dynamic light scattering essentially measures hydrodynamic radius, R_h, and it is not straightforward to obtain association number, N from R_h. The value of R_h depends on the number of water molecules in the outer shell of the micelle.

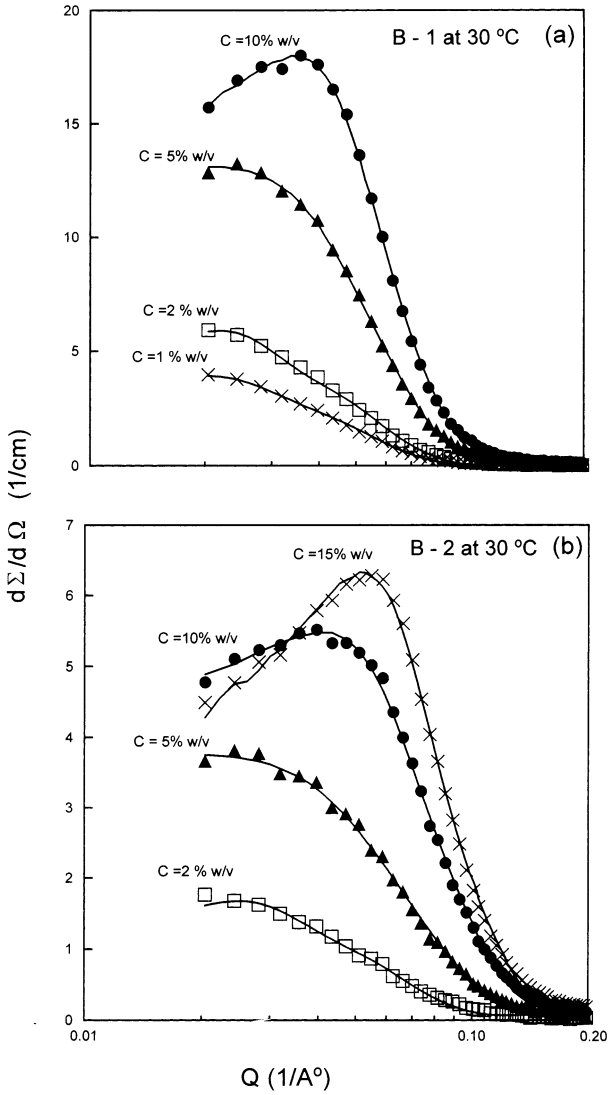

Figure 3. SANS intensity profiles for (a) B-1 and (b) B-2 copolymer aqueous solutions for different concentrations at 30 °C. Curves represent the model fitted values.

Accurate value of association number N cannot be obtained from R_h, as usually the amount of water of hydration is not known. It is thus not surprising that the use of dynamic light scattering (DLS) and SANS methods also led to differences in association number for $E_nP_mE_n$ triblock copolymer (P-85) micelles. DLS data[40] gave an association number value of 30,

TABLE 3: Values of Core Radius, R_c, Hard Sphere Radius, R_{hs}, Semiminor Axis, *a*, Semimajor Axis, *b*, Axial Ratio, *b*/*a*, Micellar Volume Fraction, ϕ, Association Number, *N*, and Number Density, ξ, for EB and EBE Copolymer Micelles in Aqueous Solution at Different Temperatures

hard sphere model						prolate ellipsoidal model						
temp (°C)	R_c (Å)	R_{hs} (Å)	ϕ	*N*	ξ (cm^{-3})	temp (°C)	*a* (Å)	*b* (Å)	*b*/*a*	ϕ	*N*	ξ (cm^{-3})
					B-1 (C = 2 wt %)							
30	43	98	0.028	318	2.368×10^{16}	50	37	136	3.7	0.069	743	1.027×10^{16}
40	49	115	0.051	458	1.644×10^{16}							
					B-2 (C = 5 wt %)							
30	34	69	0.045	142	1.219×10^{17}	50	29	75	2.6	0.071	222	0.713×10^{17}
						70	30	120	4.0	0.120	380	0.417×10^{17}

while the SANS measurements[37] for the same copolymer micelles led to a value of 116. The fact that SANS allows an independent estimation of radius of hydrophobic core R_c and one can calculate *N* from R_c using eq 12, we believe that association numbers obtained from SANS are more dependable than those obtained using DLS.

It can be seen from Figure 3a,b that the SANS intensity value systematically increases with increasing concentration for both the copolymer solutions. This increase in intensity with concentration, despite the constancy of micelle structure (within concentration limits of 1−15 wt %), can be explained by the fact that the number of micelles per unit volume would increase and hence enhance intermicellar interactions at higher copolymer concentration. As can be seen from the last column of Table 2, the number density of micelles showed a 14.7 to 15.5 times increase from 1 to 10 or 15 wt % concentrations for B-1 and B-2 copolymer micelles, respectively. Similar conclusions were also made for EPE copolymer solutions.[33,34]

For a given concentration (e.g., 5 wt %), the SANS intensity of diblock (B-1) copolymer is greater than that of triblock (B-2) copolymer (see Figure 3a,b), which indicates that micelles formed by diblock copolymers are larger in size than the triblock copolymer. This is seen in columns 2 and 3 of Table 2. Similarly the association number and number density for diblock copolymer micelles are higher than those of triblock copolymer micelles. The light scattering measurements on aqueous solutions of these two types of copolymers[15] and other range of EB and EBE copolymers[19,41] having similar overall all chain lengths showed the same trend in *N* values. In a triblock copolymer of EBE type, the core part of the micelle has two block junctions at the core/fringe interface, compared to only one constraint for a diblock copolymer. This effectively restricts the freedom of the hydrophobic chain in the core of a triblock copolymer micelle, hence resulting in associates smaller in size than those formed by diblock copolymers.

3.3.3. Temperature Dependence. The scattering curves for a fixed concentration (2 wt % for B-1 and 5 wt % for B-2) of copolymer aqueous solutions at different temperatures (40 and 50 °C for B-1, 50 and 70 °C for B-2) are shown in parts a and b of Figure 4. The method of analysis as described above, where one takes account of both P(Q) and S(Q), was used for treating those data (30 and 50 °C for B-1 and 30 °C for B-2) that show a peak. The analysis of the curves at high temperatures has been made by assuming ellipsoidal, cylindrical, and disk type shape to the P(Q) factor. The S(Q) factor at high temperatures has been set equal to unity because no correlation peak was seen in any of the curves. Out of all these, a prolate ellipsoidal model fitted very well. The micellar parameters as extracted from the prolate ellipsoidal model for copolymer associates at different temperatures are given in Table 3. It can be seen that, the minor axis *a* is invariable with the rise in temperature (50 to 70 °C for B-2), while the major axis *b* shows an increase at temperature close to the initial turbidity point.

Hamley et al.[24] have also found that a uniform sphere model fitted very well for 1 wt % aqueous solution of $E_{18}B_{10}$ copolymer at temperatures below 40 °C. At temperatures more than 40 °C, the same model could not be fitted. The authors in fact applied a worm-like micelle model for 1 wt % aqueous solution of $E_{18}B_{10}$ copolymer, avoiding the possibility of considering the prolate ellipsoidal form at high temperatures. The distortion of the spherical shape with rise in temperature is mainly attributable to the dehydration of water molecules from the core as well as the hydrated corona of the micelles. It is now well accepted[34,42−44] that dehydration effects at high temperatures not only change the conformation and size of both the hydrophobic as well as hydrophilic moieties but also enhance the association number and even further lead to great changes

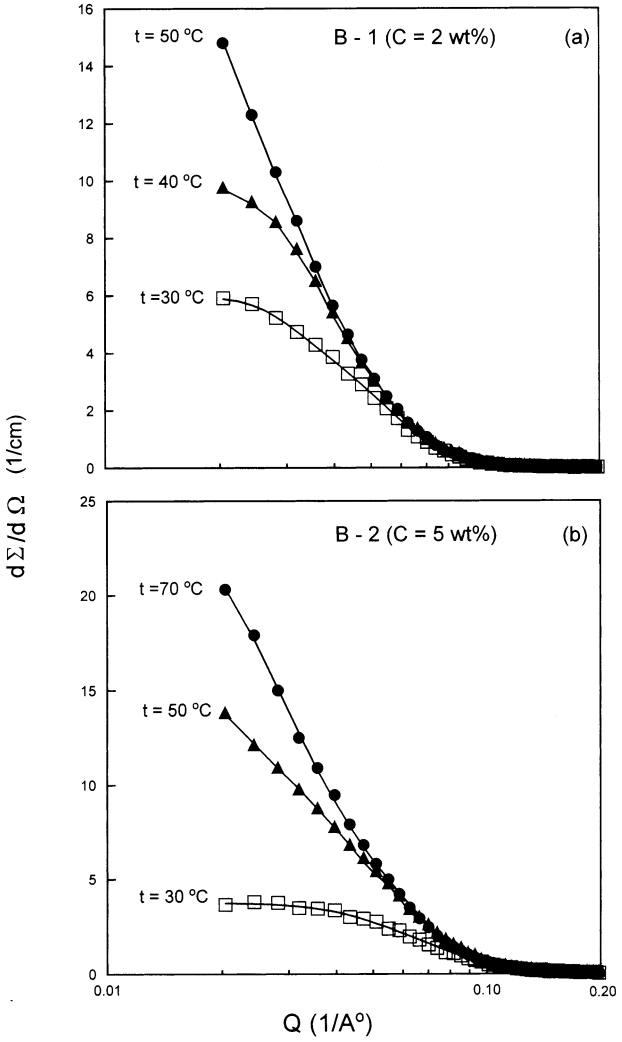

Figure 4. SANS intensity profiles for (a) 2 wt % B-1 and (b) 5 wt % B-2 copolymer aqueous solutions at different temperatures. Curves represent the model fitted values.

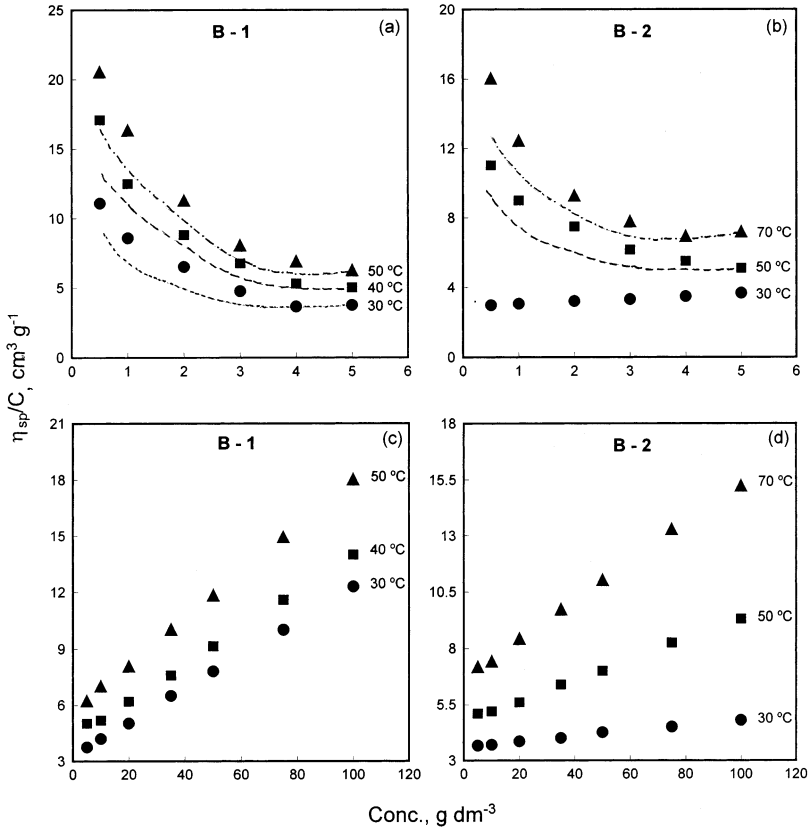

Figure 5. Concentration dependence of reduced specific viscosity for aqueous solutions of (a) and (c) for B-1 and (b) and (d) in B-2 block copolymer solutions. Points are experimental values and the dashed curves (in parts a and b) are calculated using eq 15 at respective temperatures.

in geometry. A look at Table 3, columns 3, 6, 7 corresponding to ellipsoidal model, reveals that the elongation along the major axis of the associates systematically increase N and decrease the number density of the micelles at elevated temperatures. An increase in N values indicates that more copolymer molecules have been added into the space created by the expulsion of water probably from the core and as part of the corona portion of micelles. The increase in N and the size of the micelles and decrease in hydration with increasing temperature for the same copolymers as used in the present study were also reported using light scattering measurements by Yu et al.[15] The authors, however, have assumed a spherical shape for the micelles at all temperatures and could not ascertain the information on the distortion of the shape of the micelles.

3.4. Hydration of Micelles. Viscosity measurements on micellar solutions can be used to estimate the intrinsic viscosities, $[\eta]$. The intrinsic viscosities are very handy in calculating the hydration, W, i.e., gram of water bound to gram of copolymer. The following equation has been widely used for calculating the hydration values[45,46]

$$W = \tilde{v}\rho_o\{(100\,[\eta]/2.5\tilde{v}) - 1\} \qquad (14)$$

where $\tilde{v}$, ρ_o, and $[\eta]$ are the partial specific volume of copolymer, the density of water, and the intrinsic viscosity. The partial specific volume of copolymer solute was calculated from the slope of the linear plots obtained by the equation $\rho = \rho_o + (1 - \tilde{v}\rho_o)C$, where ρ is the density of solution at a given concentration, C.

The intrinsic viscosities $[\eta]$ of the copolymer micelles were obtained by extrapolation of reduced viscosities, η_{sp}/C to zero concentrations following the Huggins procedure (i.e., fitting the η_{sp}/C data to the equation $\eta_{sp}/C = [\eta]\{1 + k_H[\eta]C\}$ where k_H = Huggins constant). Parts c and d of Figure 5 show such linear extrapolations in the concentration range 10 to 100 g dm^{-3}. Interestingly, the dependence of reduced viscosities vs concentration profiles in very dilute solutions (i.e., concentrations below 10 g dm^{-3}) showed a nonlinear curvature and the values shoot with the decrease in concentration (see Figure 5a,b) for micelles of both the copolymers. Kelarakis et al.[29] have also reported similar complex dependence of η_{sp}/C over concentration (in very dilute range and at 20 °C) for the hydroxy- and methoxy-ended $E_{18}B_{10}$ copolymers. The authors have explained the trends for low concentrations by considering the adsorption of copolymer molecules on the capillary wall of the viscometer, which in turn affects the flow time, especially with the narrow glass capillaries. The adsorption effects would increase the flow time, and hence the measured η_{sp}/C values at low concentrations are apparent. Ohrn[47] considered this effect to relate the true and apparent values of η_{sp}/C by

$$(\eta_{sp}/C)^* = \eta_{sp}/C + \Delta \quad \text{and} \quad \Delta \approx (\eta_r/C)(4a_{lay}/r) \qquad (15)$$

where * indicates apparent value. The terms a_{lay} and r in the Δ relation are the thickness of the adsorbed layer and the radius of the capillary of the viscometer used (0.300 mm in our case). Since one can equate η_r close to unity at low concentrations, true η_{sp}/C values can be estimated by changing the chosen values for adsorbed layer thickness. It has been found that values of a_{lay} equal to 0.0002, 0.0003, and 0.0005 mm at 30, 40, 50 °C for B-1 the diblock copolymer and 0.0002 and 0.0004 mm at 50 and 70 °C for the B-2 triblock copolymer reproduced the trends in reduced viscosity vs concentration profiles at low concentration. Another interesting feature is that as the % of B is decreased from 45 to 40 from B-1 to B-2, the nonlinear trends in the above profiles appeared at high temperatures. Thus it

TABLE 4: Partial Specific Volume, $\tilde{v}$, Intrinsic Viscosities, [η], and Hydration of Copolymer Micelles, *W*, in Aqueous Solutions at Different Temperatures

temp (°C)	$\tilde{v}$ (mL g^{-1})	[η] (cm^3 g^{-1})	*W* [g(water)/ g(copolymer)]	H_2O/single molecule
		B-1		
25	0.9316	3.8	1.69	150
30	0.9371	3.6	1.65	147
35	0.9426	3.4	1.60	142
40	0.9479	4.6	1.54	137
45	0.9589	5.3	1.30	116
50	0.9671	6.0	1.28	114
		B-2		
25	0.9021	3.0	1.40	148
30	0.9145	3.2	1.28	135
45	0.9254	4.1	1.16	122
50	0.9310	4.3	1.14	120
55	0.9359	4.5	1.13	119
60	0.9411	5.1	1.10	116
65	0.9463	5.8	1.04	110
70	0.9615	6.9	0.90	95

can be rationalized that the adsorption effects, as expected, would be dominant in very dilute solutions at elevated temperatures and in copolymers with more content of B.

The intrinsic viscosities as obtained from linear plots shown in Figure 5c,d range mostly from 3 to 4.1 cm^3 g^{-1} up to temperature limits of 40−45 °C, and hence the micelles are near to hard spheres as defined by Einstein's equation $[\eta] = 2.5/\rho$ where ρ is close to 1 g cm^{-3} in the present case. However, beyond the temperature of 40 °C (for B-1) and 45 °C (for B-2), [η] values showed about two-fold increase (or more), indicating the distortion of the hard spherical shape for the micelles at elevated temperatures.

The estimated values of $\tilde{v}$ and *W* at different temperatures are listed in Table 4. The hydration values show a gradual decrease with increase in the temperature. Our observed 1.3× and 1.6× decrease in the extent of hydration for B-1 (25−50 °C) and B-2 (25−70 °C) are comparable with the 1.4× and 1.7× decrease in hydration of the same copolymers as estimated from light scattering measurements.[15] The light scattering measurements on micelles of E_mB_n and $E_mB_nE_m$ copolymers[17,19,41] in aqueous solutions showed that both the hydrodynamic and the core radii increase and hydration decreases with the rise in the temperature (i.e., dehydration is responsible for increase in the size of the micelles). Similarly, SANS measurements on $E_{86}B_{10}$ micelles[23] in D_2O, as analyzed in terms of a core−shell model employing hard sphere interaction potential, also revealed that both the hard sphere and core radii increase and hydration decreases at elevated temperatures.

4. Conclusions

$E_{18}B_9$ and $E_{13}B_{10}E_{13}$ di- and triblock copolymers form micelles of spherical shape in water at 30 °C. The CMC values and the molecular areas at the water/air interface for the triblock copolymer are higher than for the diblock copolymer. The micellar size and shape of both diblock and triblock copolymer micelles have been found to be unaltered in the concentration range 1−15 wt % at 30 °C. Diblock $E_{18}B_9$ copolymer micelles have larger size and association numbers than the triblock $E_{13}B_{10}E_{13}$ copolymer micelles. The micellar volume fraction and the number density of micelles increase with the increase in concentration at 30 °C for the micelles of both the copolymers indicating enhanced inter micellar interactions. Micelles of both the di- and triblock copolymers undergo sphere-to-ellipsoidal transition at elevated temperatures. The distortion of the shape and the elongation of micelles at elevated temperatures coincided with the dehydration of both hydrophobic polyoxybutylene core and hydrophilic polyoxyethylene corona parts.

Acknowledgment. We thank the IUC and Department of Atomic Energy, India, for the financial support under Grant no. IUC/CRS-M-73/362-66. We also thank Dr. B. A. Dasannacharya for his useful suggestions and interest in the work.

References and Notes

(1) Booth, C.; Attwood, D. *Macromol. Rapid. Commun.* **2000**, *21*, 501.
(2) Alexandridis, P. *Curr. Opin. Colloid Interface Sci.* **1997**, *2*, 478.
(3) Chu, B.; Zhou, Z. Physical Chemistry of Polyalkylene Block Copolymer Surfactants. In *Nonionic Surfactants*; Nace, V. M., Ed.; Marcel Dekker: New York, 1996; Surfactant Science Series, Vol. 60, p 67.
(4) Almgren, M.; Brown, W.; Hvidt, S. *Colloid Polym. Sci.* **1995**, *273*, 2.
(5) Altinok, H.; Nixon, S. K.; Gorry, P. A.; Attwood, D.; Booth, C.; Kelarakis, A.; Havredaki, V. *Colloids Surf. B* **1999**, *16*, 73.
(6) Altinok, H.; Yu, G.-E.; Nixon, S. K.; Gorry, P. A.; Attwood, D.; Booth, C. *Langmuir* **1997**, *13*, 5837.
(7) Nace, V. M. *J. Am. Oil Chem. Soc.* **1996**, *73*, 1.
(8) Yang, L.; Bedells, A. D.; Attwood, D.; Booth, C. *J. Chem. Soc., Faraday Trans.* **1992**, *88*, 1447.
(9) Yang, Z.; Pousia, E.; Heatley, F.; Price, C.; Booth, C.; Castelletto, V.; Hamley, I. W. *Langmuir* **2001**, *17*, 2106.
(10) Heatley, F.; Yu, G.-E.; Sun, W.-B.; Pywell, E. J.; Mobbs, R. H.; Booth, C. *Eur. Polym. J.* **1990**, *26*, 583.
(11) Nace, V. M.; Whitmarch, R. H.; Edens, M. W. *J. Am. Oil Chem. Soc.* **1994**, *7*, 777.
(12) *B-Series Polyglycols, Butylene Oxide/Ethylene Oxide Block Copolymers*, technical literature; Dow Chemical Co.: Freeport, TX, 1994.
(13) Yang, Z.; Pickard, S.; Deng, N.-J.; Barlow, R. J.; Attwood, D.; Booth, C. *Macromolecules* **1994**, *27*, 2371.
(14) Yang, Y.-W.; Deng, N.-J.; Yu, G.-E.; Zhou, Z.-K.; Attwood, D.; Booth, C. *Langmuir* **1995**, *11*, 4703.
(15) Yu, G.-E.; Yang, Y.-W.; Yang, Z.; Attwood, D.; Booth, C.; Nace, V. M. *Langmuir* **1996**, *12*, 3404.
(16) Zhuo, Y.; Yang, Y.-W.; Zhou, Z.-K.; Attwood, D.; Booth, C. *J. Chem. Soc., Faraday Trans.* **1996**, *92*, 257.
(17) Yu, G.-E.; Mistry, D.; Ludhera, S.; Heatley, F.; Attwood, D.; Booth, C. *J. Chem. Soc., Faraday Trans.* **1997**, *93*, 3383.
(18) Kelarakis, A.; Havredaki, V.; Yu, G.-E.; Derici, L.; Booth, C. *Macromolecules* **1998**, *31*, 944.
(19) Chaibundit, C.; Mai, S.-M.; Heatley, F.; Booth, C. *Langmuir* **2000**, *16*, 9645.
(20) Bedells, A. D.; Arafeh, R. M.; Yang, Z.; Attwood, D.; Heatley, F.; Pedget, J. C.; Price, C.; Booth, C. *J. Chem. Soc., Faraday Trans.* **1993**, *89*, 1235.
(21) Luo, Y.-Z.; Nicholas, C. V.; Attwood, D.; Collett, J. H.; Price, C.; Booth, C. *Colloid Polym. Sci.* **1992**, *270*, 1094.
(22) Luo, Y.-Z.; Nicholas, C. V.; Attwood, D.; Collett, J. H.; Price, C.; Booth, C.; Zhou, Z.-K.; Chu, B. *J. Chem. Soc., Faraday Trans.* **1993**, *89*, 539.
(23) Derici, L.; Ledger, S.; Mai, S.-M.; Booth, C.; Hamley, I. W.; Pedersen, J. S. *Phys. Chem. Chem. Phys.* **1999**, *1*, 2773.
(24) Hamley, I. W.; Pedersen, J. S.; Booth, C.; Nace, V. M. *Langmuir* **2001**, *17*, 6386.
(25) Jain, D. V. S.; Singh, S. *Ind. J. Chem.* **1972**, *10*, 629.
(26) Reddick, J. A.; Bunger, W. B.; Sakano, T. K. *Organic Solvents*, 4th ed.; Wiley Interscience: New York, 1986; Vol. II.
(27) Aswal, V. K.; Goyal, P. S. *Curr. Sci.* **2000**, *79*, 947.
(28) Rosen, M. J. *Surfactants and Interfacial Phenomena*, 2nd ed.; Wiley: New York, 1989; p 67.
(29) Kelarakis, A.; Havredaki, V.; Booth, C.; Nace, V. M. *Macromolecules* **2002**, *35*, 5591.
(30) Alexandridis, P.; Athanassiou, V.; Fukuda, S.; Hatton, T. A. *Langmuir* **1994**, *10*, 2604.
(31) (a) Chen, S. H. *Annu. Rev. Phys. Chem.* **1986**, *37*, 351. (b) Chen, S. H.; Lin, T. L. *Methods of Experimental Physics*; Academic Press: New York, 1987; Vol. 23 B, p 489.
(32) Hayter, J. B.; Penfold, J. *Colloid Polym. Sci.* **1983**, *261*, 1022. Hayter, J. B.; Penfold, J. *Mol. Phys.* **1981**, *42*, 109. Hayter, J. B.; Penfold, J. *Mol. Phys.* **1982**, *46*, 109. Hayter, J. B.; Penfold, J. *J. Chem. Soc., Faraday Trans. 1* **1981**, *77*, 1851.
(33) Mortensen, K.; Talmon, Y. *Macromolecules* **1995**, *28*, 8829.
(34) Jain, N. J.; Aswal, V. K.; Goyal, P. S.; Bahadur, P. *J. Phys. Chem.* **1998**, *102*, 8452.
(35) Guinier, A.; Fournet, G. *Small Angle Scattering of X-rays*; Wiley: New York, 1955.

(36) Percus, J. K.; Yevick, G. J. *Phys. Rev.* **1958**, *110*, 1.
(37) Mortensen, K.; Pedersen, J. S. *Macromolecules* **1993**, *26*, 805.
(38) Ashcroft, N. W.; Leckner, J. *Phys. Rev.* **1966**, *83*, 145.
(39) Kinning, D. J.; Thomas, E. L. *Macromolecules* **1984**, *17*, 712.
(40) Brown, W.; Schillen, K.; Almgren, M.; Hvidt, S.; Bahadur, P. *J. Phys. Chem.* **1991**, *95*, 1850.
(41) Mingvanish, W.; Mai, S.-M.; Heatley, F.; Booth, C.; Attwood, D. *J. Phys. Chem. B* **1999**, *103*, 11269.
(42) Goldmints, I.; von Gottberg, F. K.; Smith, K. A.; Hatton, T. A. *Langmuir* **1997**, *13*, 3659.
(43) Goyal, P. S.; Menon, S. V. G.; Dasannacharya, B. A.; Thiyagarajan, P. *Phys. Rev. E* **1995**, *51*, 2308.
(44) Liu, Y. C.; Chen, S. H.; Huang, J. S. *Physica B* **1998**, *243*, 1019.
(45) Tokiwa, F.; Ohki, K. *J. Phys. Chem.* **1967**, *71*, 1343.
(46) Oncley, J. L. *Ann. N.Y. Acad. Sci.* **1949**, *41*, 121.
(47) Ohrn, O. E. *J. Polym. Sci.* **1955**, *17*, 137.